Int. J. Electrochem. Sci., 7 **(2012)** 3959 - 3981

International Journal of ELECTROCHEMICAL SCIENCE
www.electrochemsci.org

Green Approach to Corrosion Inhibition of Mild Steel by Essential Oil Leaves of *Asteriscus Graveolens* (Forssk.) in Sulphuric Acid Medium

M. Znini[1], *G. Cristofari*[2], *L. Majidi*[1,*], *A. Ansari*[1], *A. Bouyanzer*[3], *J. Paolini*[2], *J Costa*[2], *B. Hammouti*[3]

[1] Université Moulay Ismail, Laboratoire des Substances Naturelles & Synthèse et Dynamique Moléculaire, Faculté des Sciences et Techniques, Errachidia, Morocco.
[2] Université de Corse, Laboratoire de Chimie des Produits Naturels, UMR CNRS 6134, Faculté des Sciences et Techniques, Corse, France.
[3] Université Mohamed Premier, Laboratoire de Chimie Appliquée et Environnement, Faculté des Sciences, Oujda, Morocco.
[*]E-mail: lmajidi@yahoo.fr

Received: 22 March 2012 / *Accepted:* 13 April 2012 / *Published:* 1 May 2012

Essential oil of leaves of *Asteriscus graveolens* was obtained by hydrodistillation and analyzed by GC, GC/MS and ^{13}C NMR. Twenty-seven compounds were identified amounting to 98.1% of the total oil. This essential oil was characterized by having a high content of oxygenated sesquiterpenes (93.3%) with 6-oxocyclonerolidol 19 (74.9%) and 6-hydroxycyclonerolidol 23 (11.8%) are the major components. The inhibition of the corrosion of mild steel in sulphuric acid solution by *Asteriscus graveolens* essential oil has been studied using weight loss measurements, electrochemical polarization and EIS methods. Inhibition was found to increase with increasing concentration of the essential oil to attain 82.89% at 3g/L. Polarisation curves revealed that this oil act as mixed type inhibitor with a strong predominance of anodic character. The effect of temperature, immersion time on the corrosion behaviour of mild steel in 0.5M H_2SO_4 without and with the *A. graveolens* oil at 3 g/L was also studied. The associated activation energy has been determined. The inhibition was assumed to occur via physical adsorption of the inhibitor molecules on the metal surface. The adsorption of inhibitor onto the mild steel surface was found to be a spontaneous process and to follow the Langmuir adsorption isotherm.

Keywords: *Asteriscus graveolens*, Hydrodistillation, Essential oil, Mild steel, Corrosion inhibition

1. INTRODUCTION

Mild steel has found wide applications in a broad spectrum of industries and machinery; however its tendency to corrosion made it not the adequate for exposures in contact with aggressive

acids [1]. Sulphuric acid, for example, is often used as a pickling acid for mild steel to remove undesirable corrosion products. Nevertheless, the chemical acid cleaning will cause metal corrosion upon the already cleaned surface after the elimination of the corrosion products [2]. To overcome this problem, the efforts are deployed to stop or delay to the maximum the attack of metals in various corrosive media. Indeed, the use of inhibitors is one of the best methods of protecting metals against corrosion. Most corrosion inhibitors are synthetic organic compounds having hetero atoms in their aromatic or long carbon chain [3]. These organic compounds can adsorb on the metal surface, block the active sites on the surface and thereby reduce the corrosion rate. However, the toxic effects of most synthetic corrosion inhibitors, the obligations of health and human security have led to the research of green alternatives that are environmentally friendly and harmless [3]. Thus, the researches have been focused on the use of eco-friendly compounds and ecologically acceptable such as extract of common plants because to bio-degrability, eco-friendliness, low cost and easy availability and renewable sources of materials [4].

Recently, several studies have been carried out on the inhibition of corrosion of metals by plant extract especially essential oils. In this context, our laboratory adopted a strategy of evaluation of this molecules against corrosion of mild steel in acid media, thus, we previously reported that essential oils of *Salvia aucheri* var. *mesatlantica* [5], *Mentha spicata* [6], *Warionia saharea* [7], *Lavandula multifida* [8], *Pulicaria mauritanica* [9], *Mentha pulegium* [10], *Eucalyptus globulus* [11], *Artemisia herba-alba* [12], *Cedrus atlantica* [13] and *Foeniculum vulgaris* [14] have been found to be very efficient corrosion inhibitors for mild steel in acid media. In this paper, our choice is focused to essential oil of *Asteriscus graveolens* (Forssk.) Less.

Figure 1. *Asteriscus graveolen* (Forssk.) in its native habitat in south-eastern of Morocco

Asteriscus graveolens (Forssk.) Less. (syn. *Bubonium graveolens*, *Odontospermum graveolens* or *Nauplius graveolens*) (Fig. 1), is an endemic aromatic plant mainly distributed in southeastern Morocco [15]. It is present throughout the Sahara especially in sandy clay pans but also on the trays and it blooms in spring, from March to May. It is locally known as 'Tafss' [15], and has been used in Sahara folk medicine as a stomachic, for treating fever, gastrointestinal tract complaints, cephalic pains, bronchitis and as an anti-inflammatory [16], but handling plant may cause skin irritation or allergic reaction. This plant is also used in Morocco for its antimicrobial [17], antifungal [18] and hypoglycemic [19] properties. The plants of this genus are known to produce compounds with potential antitumor, antispasmodic, anti-inflammatory activities and are known also for the treatment of infected wounds [20].

The aim of this study was to obtain for the first time information on the chemical composition of *Asteriscus graveolens* essential oil and its inhibitory effect on the corrosion of mild steel in 0.5 M H_2SO_4 using gravimetric and electrochemical methods.

2. EXPERIMENTAL DETAILS

2.1. Plant material

The leaves of *Asteriscus graveolens* were harvested in March 2009 (full bloom) Mellab (Errachidia) located at the south-east of Morocco. Voucher specimen was deposited in the herbarium of Faculty of Sciences of and Technology of Errachidia (Marocco).

2.2. Essential oil isolation

The dried vegetal material (100 g) were water-distillated (3h) using a Clevenger-type apparatus according to the method recommended in the European Pharmacopoeia [21] and the essential oil yields were of around 0.6% for the leaves parts.

2.3. Oil fractionation

The leaves essential oil of *A. graveolens* (1 g) was chromatographed by an Automatised Flash Chromatography CFA system (TeledyneE Isco, Lincoln) using normal phase silica (12 g, 15-40 µ, 60 Å). The apolar fraction A was eluted with hexane (n-C_6H_{14}) and the polar fractions P with a mixture of diisopropyloxyde $(C_3H_7)_2O$/hexane of increasing polarity (Fig. 2). The elution gradient % $(C_3H_7)_2O$/n-C_6H_{14} (time) was: 0% (3 min) ; 1% (5 min) ; 2% (5 min) ; 2.5% (7 min) ; 3.5% (5 min) ; 5% (5 min) ; 5-100% (5 min) and 100% (3 min). The oil fractionations lead to one apolar fraction and 14 polar fractions ($P_{1\text{-}14\ leaves}$).

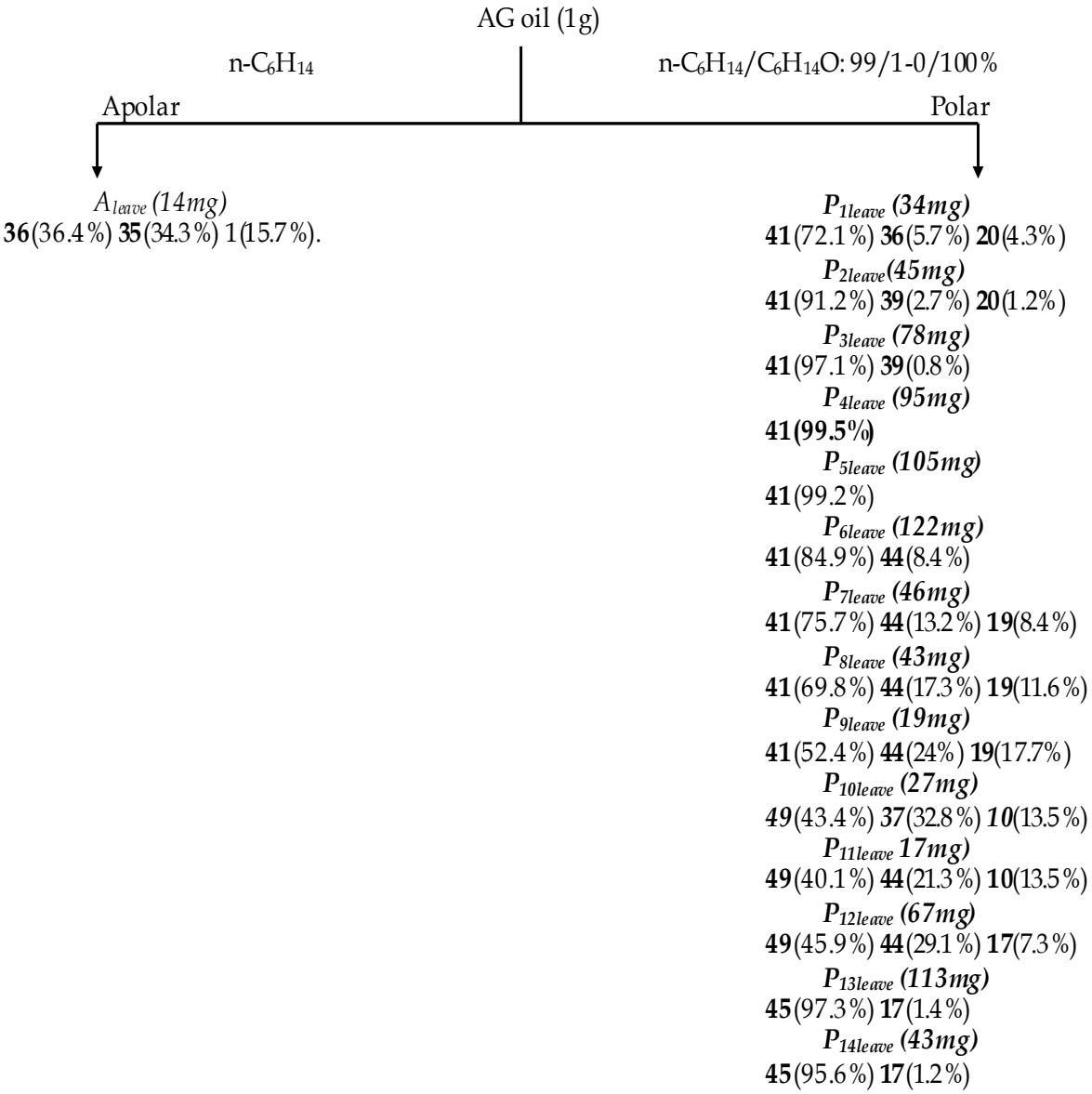

Figure 2. Fractionation of leaves essential oil of *A.graveolens*.

2.4. GC analysis

GC analyses were carried out using a Perkin-Elmer Autosystem (Waltham, MA, USA) XL GC apparatus equipped with dual flame ionization detectors (FID) and fused-silica capillary columns (60 m x 0.22 mm i.d.; film thickness 0.25µm) coated with Rtx-1(polydimethylsiloxane) and Rtx-wax (polyethyleneglycol). The oven temperature was programmed from 60 to 230 °C at 2 °C/min and the held at 230 °C for 35 min. Injector and detector temperatures were maintained at 280 °C. Samples were injected in the split mode (1/50) using helium as carrier gas (1 mL/min); the injection volume of pure oil was 0.1 µL. Retention indices (RI) of compounds were determined relative to the retention times of series of n-alkanes (C5-C30), using the Van den Dool and Kratz equation [22].

2.5. GC-MS analysis

Samples were analysed with a Perkin-Elmer Turbo mass detector (quadrupole), coupled to Perkin-Elmer Autosystem XL chromatograph equipped with Rtx-1 and Rtx-wax fused-silica capillary columns. The carrier gas was helium (1mL/min), the ion source temperature was 150°C, the oven temperature was programmed from 60 to 230 °C at 2 °C/min and the held at 230 °C for 35 min, the injector was operated in the split (1/80) mode at a temperature of 280 °C, the injection volume was 0.2 µL of pure oil, the ionization energy was 70 eV, EI/MS were acquired over the mass range 35-350 Da.

2.6. NMR analysis

All NMR spectra were recorded on a Bruker Avance (Wissembourg, France) 400 Fourrier Transform spectrometer equipped with a 5 mm probe and operating at 100.13 MHz for ^{13}C-NMR. Compounds were dissolved in deuterated chlorofform and all shifts referred to the internal standard tetramethylsilane (TMS). ^{13}C-NMR spectra were recorded with the following parameters: pulse with 4 µs (flip angle 45°); acquisition time 2.7 s for 128 K data with a spectral width of 25 000 Hz (250 ppm); CPD mode decoupling; digital resolution 0.183 Hz/pt. The number of accumulated scans was 5000 for each sample (containing ca. 40 mg of oil in 0.5 ml of deuterochloroform) Exponential line broadening multiplication (1 Hz) of the free induction decay was applied prior to Fourier transformation.

2.7. Identification of essential oil constituents

The identification of the components was based on:

(i) A comparison between calculated retention indices on polar (RIp) and apolar (RIa) columns with those of pure standard authentic compounds and literature data [22,23];

(ii) A comparison of Mass Spectra with those of our own library of authentic compounds and with those of commercial library [23,24].

2.8. Quantification of essential oil constituents

The quantification of essential oil components was carried out using the methodology reported by Bicchi et al. [25] and modified as follows. Response factors (RF) of 29 standard compounds grouped into seven chemical groups (monoterpene hydrocarbons, sesquiterpene hydrocarbons, alcohols, ketones, aldehydes, esters, others) were measured by GC (Table 1). RFs and calibration curves were determined by diluting each standard in hexane, at five concentrations, containing tridecane (final concentration 0.7 g/100 g) as internal standard. Analysis of each standard was performed in triplicate. For quantification of essential oil components, tridecane (0.2 g/100 g) was added as internal standard in essential oil. The correction factors (averages of response factors from standards) of each chemical group were calculated and used to determine the essential oil component concentrations (g/100 g) according to their chemical group.

Table 1. Measurement of response factors (RFs) of the different chemical groups (SD: standard deviation).

Compounds	RF±SD
Monoterpene hydrocarbons	1.01±0.05
neo-allo-Ocimene	1.00±0.01
α-Pinene	1.04±0.01
β-Pinene	1.08±0.01
γ-Terpinene	1.01±0.01
Limonene	0.94±0.01
Sesquiterpene hydrocarbons	1.00±0.03
β-Caryophyllene	0.98±0.01
α-Humulene	1.01±0.01
Aromadendrene	1.03±0.01
Aromatic hydrocarbon	0.93±0.04
p-cymene	0.93±0.04
Alcohols	1.34±0.04
Nerol	1.31±0.02
Lavandulol	1.32±0.02
Cedrol	1.31±0.02
Globulol	1.34±0.02
(E)-3-Hexen-1-ol	1.40±0.02
Aldehydes	1.40±0.02
(E)-2-Hexenal	1.39±0.01
(E,E)-2,4-Decadienal	1.42±0.01
(E)-2-Decenal	1.40±0.01
Ketones	1.30±0.02
Artemisia ketone	1.30±0.01
decan-2-one	1.28±0.03
Camphor	1.31±0.01
Jasmone	1.32±0.01
Esters	1.55±0.03
Pentyl acetate	1.53±0.01
Lavandulyl acetate	1.54±0.01
trans-Myrtenyl acetate	1.53±0.01
Cedryl acetate	1.59±0.01
Others	
Caryophyllene oxide	1.59±0.01
Isoborneol methyl ether	1.25±0.01
1,8-cinéole	1,25±0,01
Carvacrol methyl ether	1.23±0.01

2.9. Corrosion test

2.9.1. Weight loss measurements

The aggressive solution (0.5M H_2SO_4) was prepared by dilution of Analytical Grade 98% H_2SO_4 with double-distilled water. Prior to all measurements, the mild steel samples (0.09% P; 0.38% Si; 0.01% Al; 0.05% Mn; 0.21% C; 0.05% S and the remainder iron) were polished with different emery paper up to 1200 grade, washed thoroughly with double-distilled water, degreased with AR grade ethanol, acetone and drying at room temperature. Gravimetric measurements were carried out in a double walled glass cell equipped with a thermostat-cooling condenser. The solution volume was 100 mL with and without the addition of different concentrations of *Asteriscus graveolens* (AG) oil ranging from 0.25 g/L to 3 g/L. The mild steel specimens used had a rectangular form (2 cm x 2 cm). The immersion time for the weight loss was 6 h at 298 K.

After the corrosion test, the specimens of steel were carefully washed in double-distilled water, dried and then weighed. The rinse removed loose segments of the film of the corroded samples. Duplicate experiments were performed in each case and the mean value of the weight loss is reported. Weight loss allowed us to calculate the mean corrosion rate as expressed in $mg.cm^{-2}\ h^{-1}$.

The corrosion rate (W) and inhibition efficiency Ew (%) were calculated according to the Eqs. (1) and (2) respectively:

$$W = \frac{\Delta m}{S.t} \qquad (1)$$

$$E_w\,\% = \frac{W_{corr} - W_{corr(inh)}}{W_{corr}} \times 100 \qquad (2)$$

where Δm (mg) is the specimen weight before and after immersion in the tested solution, W_{corr} and $W_{corr(inh)}$ are the values of corrosion weight losses ($mg/cm^2.h$) of mild steel in uninhibited and inhibited solutions, respectively, S is the area of the mild steel specimen (cm^2) and t is the exposure time (h).

2.9.2. Polarization and EIS measurements

Electrochemical measurements were carried out in a conventional three-electrode electrolysis cylindrical Pyrex glass cell. The working electrode (WE) in the form of disc cut from steel has a geometric area of 1 cm^2 and is embedded in polytetrafluoroethylene (PTFE). A saturated calomel electrode (SCE) and a disc platinum electrode were used respectively as reference and auxiliary electrodes, respectively.

The temperature was thermostatically controlled at 298 ± 1K. The WE was abraded with silicon carbide paper (grade P1200), degreased with AR grade ethanol and acetone, and rinsed with double-distilled water before use.

Running on an IBM compatible personal computer, the 352 Soft Corr^{TM} III Software communicates with EG&G Instruments potentiostat–galvanostat model 263A at a scan rate of 0.5 mV/sec. Before recording the cathodic polarisation curves, the mild steel electrode is polarised at -800 mV for 10 min.

For anodic curves, the potential of the electrode is swept from its corrosion potential after 30 min at free corrosion potential, to more positive values.

The test solution is deaerated with pure nitrogen. Gas bubbling is maintained through the experiments.

In the case of polarization method the relation determines the inhibition efficiency (E_I %):

$$E_I\,\% = \frac{I_{corr} - I_{corr(inh)}}{I_{corr}} \times 100 \qquad (3)$$

where I_{corr} and $I_{corr\ (inh)}$ are the corrosion current density values without and with the inhibitor, respectively, determined by extrapolation of cathodic and anodic Tafel lines to the corrosion potential.

The electrochemical impedance spectroscopy (EIS) measurements were carried out with the electrochemical system which included a digital potentiostat model Volta lab PGZ 100 computer at E_{corr} after immersion in solution without bubbling, the circular surface of mild steel exposing of 1 cm^2 to the solution were used as working electrode.

After the determination of steady-state current at a given potential, sine wave voltage (10 mV) peak to peak, at frequencies between 100 kHz and 10 mHz were superimposed on the rest potential. Computer programs automatically controlled the measurements performed at rest potentials after 30 min of exposure.

The impedance diagrams are given in the Nyquist representation. Values of R_t and C_{dl} were obtained from Nyquist plots.

The charge-transfer resistance (R_t) values are calculated from the difference in impedance at lower and higher frequencies, as suggested by Tsuru and al. [26]. The inhibition efficiency got from the charge-transfer resistance is calculated by the following relation:

$$E_{Rt}\,\% = \frac{R'_t - R_t}{R'_t} \times 100 \qquad (4)$$

R_t and R'_t are the charge-transfer resistance values without and with inhibitor respectively. R_t is the diameter of the loop.

The double layer capacitance (C_{dl}) and the frequency at which the imaginary component of the impedance is maximal ($-Z_{max}$) are found as represented in Eq. (5):

$$C_{dl} = \frac{1}{\omega . R_t} \quad \text{where } \omega = 2\,\pi\,.\,f_{max} \qquad (5)$$

Impedance diagrams are obtained for frequency range 100 KHz –10 mHz at the open circuit potential for mild steel in 0.5 M H_2SO_4 in the presence and absence of AG oil.

2.10. Effect of temperature

The effect of temperature on the inhibited acid–metal reaction is very complex, because many changes occur on the metal surface such as rapid etching, desorption of inhibitor and the inhibitor itself may undergo decomposition [27]. The change of the corrosion rate at 3 g/L of the AG oil during 2 h of immersion with the temperature was studied in 0.5 M H_2SO_4, both in the absence and presence of AG oil. For this purpose, gravimetric experiments were performed at different temperatures (303–343 K).

To calculate activation thermodynamic parameters of the corrosion process, Arrhenius Eq. (6) and transition state Eq. (7) were used [28]:

$$W = A \exp\left(\frac{-Ea}{RT}\right) \quad (6)$$

$$W = \frac{RT}{Nh} \exp\left(\frac{\Delta S^{\circ}_{a}}{R}\right) \exp\left(-\frac{\Delta H^{\circ}_{a}}{RT}\right) \quad (7)$$

where Ea is the apparent activation corrosion energy, R is the universal gas constant, A is the Arrhenius pre-exponential factor, h is the Plank's constant, N is the Avogrado's number, $\Delta S°_a$ is the entropy of activation and $\Delta H°_a$ is the enthalpy of activation.

3. RESULTS AND DISCUSSION

2.1. Essential oil composition

The analysis of the *A. graveolens* essential oil was carried out by GC, and GC–MS, using the methodologies described in the section 2. Twenty-seven components were identified in the essential oils (Table 2).

The component concentrations (g/100 g of essential oil) were determined using the correction factors of each chemical group (i.e., the average of the response factors (RFs) from standards) according to the methodology described in experimental section.

Among them, five hydrocarbons (0.9%), twenty-one oxygenated terpenic compounds (97%) and one acyclic non-terpenic component 2 (0.2%) were identified in the essential oil of *A. graveolens*, amounting to 98.1% of the total oil. This oil was characterized in having a high content of oxygenated sesquiterpenes (93.3%) with 6-oxocyclonerolidol 19 (74.9%) and 6-hydroxycyclonerolidol 23 (11.8%) are the major components. After oil fractionation by CFA (Fig. 2), the structure of components 19 and 23 was confirmed by analysis of ^{13}C NMR chemical shifts of fraction $P_{4\ leave}$ (19: 99.2%) and $P_{13\ leave}$ (23: 97.3%) (Fig. 3).

Table 2. Chemical composition of *A. graveolens* leaves essential oil from Morocco

N a	Components	Ir a b	Ir p c	Component concentration (g/100g) d
1	α-pinene	933	1004	0.1
2	6-methylhept-5-en-2-one	980	1302	0.2
3	1,8-cineol	1023	1183	0.1
4	Linalool	1081	1544	0.5
5	α-thujone	1090	1384	0.2
6	α-campholenal	1108	1446	0.1
7	Camphor	1124	1470	0.5
8	terpinen-4-ol	1162	1580	0.1
9	α-terpineol	1170	1700	0.2
10	Estragole	1177	1650	tr
11	Carvotanacetone	1218	1664	0.5
12	(Z)-chrysanthenyl acétate	1248	1526	0.3
13	Carvacrol	1279	2135	0.7
14	α-humulene	1452	1628	0.1
15	γ-cadinene	1504	1737	0.1
16	δ-cadinene	1518	1705	0.1
17	(Z)-nerolidol	1522	1518	0.3
18	Kessane	1528	1715	0.5
19	6-oxocyclonerolidol	1555	1969	74.9
20	(Z)-8 acetoxy chrysanthenyl acetate	1564	2122	0.5
21	Caryophyllene oxyde	1576	1921	0.1
22	Humulene II époxyde	1598	1975	1.4
23	6-hydroxycyclonerolidol ¤	1622	2246	11.8
24	τ-cadinol	1631	2102	0.5
25	β-eudesmol	1636	2160	1
26	Intermedeol	1643	2160	3.2
27	α-oxobisabolene¤	1707	2266	0.1
Total				98.1
Monoterpene hydrocarbons				0.1
Sesquiterpene hydrocarbons				0.8
Oxygenated monoterpenes				3.7
Oxygenated sesquiterpenes				93.3
acyclic non-terpenic (2)				0.2

a The numbering refers to elution order on apolar column (Rtx-1)
b RIa = retention indices measured on the apolar column (Rtx-1)
c RIp = retention indices measured on the polar column (Rtx-Wax)
d Concentration of components (g/100 g) are calculated using Response Factors RFs according to their chemical group (see Table 1) and based on GC peak areas on the apolar column (Rtx-1) tr= trace (<0.05%)

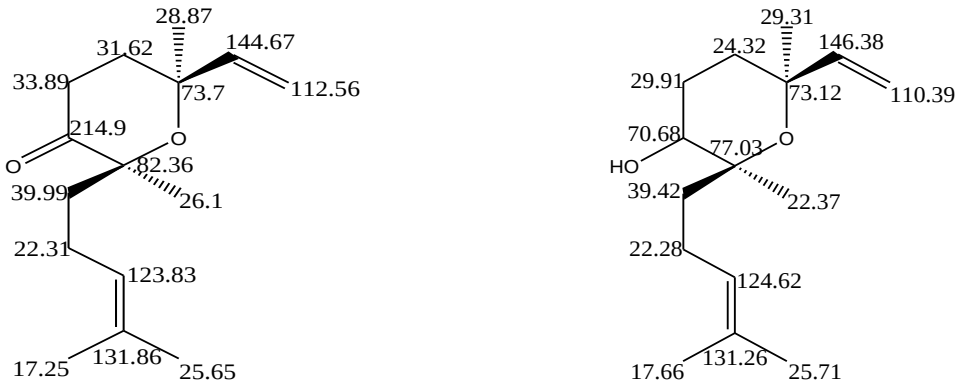

6-oxocyclonerolidol 19 6-hydroxycyclonerolidol 23

Figure 3 . Chemical molecular structures and ^{13}C NMR chemical shifts of 6-oxocyclonerolidol 19 and 6-hydroxycyclonerolidol 23

To our knowledge, only two studies have been published concerning the chemical composition of *A. graveolens* essential oil under synonyms. Then Cheriti et al. [15] studied the chemical composition of essential oil of leaves and flowers from *Bubonium graveolens* from the South-Western Algeria. Analysis were carried out using GC and GC/MS; 1,8-cineole and δ-cadinol were reported as major constituents in both organs. According to these authors [15], the flower essential oil was characterized by a high relative abundance of 2,6-dimethylhepta-1,6-dien-4-yl acetate and (E)-chrysanthenyl acetate while the presence of δ-cadinene was reported only in the leaf essential oil. The second corresponding to flowering parts of *Nauplius graveolens* collected in Sinai (Egypt) [16]**.** 49 compounds were identified by GC/MS and the major components were 2-(2-keto-4-methylcyclohexyl)-6,7-dimethyl-l,5-hydroxy-3,5-octadiene, α-pinene, cedrenol, α-phellandrene and α-himachalene.

3.2. Corrosion tests

3.2.1. Weight loss measurements

The effect of addition of *A. graveolens* essential oil (AG oil) tested at different concentrations on the corrosion of mild steel in 0.5M H_2SO_4 solution was studied by weight loss measurements at 298 K after 6 h of immersion period.

The values of percentage inhibition efficiency Ew (%) and corrosion rate (W) obtained from weight loss method at different concentrations of AG oil at 298 K are summarized in Table 3.

It is very clear that the AG oil inhibits the corrosion of mild steel in 0.5M H_2SO_4 solution, at all concentrations used in this study, and the corrosion rate (W) decreases continuously with increasing concentration of natural oil at 298 K. Indeed, Fig. 4 shown that the corrosion rate values of mild steel decrease when the inhibitor concentration increases while Ew (%) values of AG oil increase with the increase of the concentration reaching a maximum value of 82.89% at a concentration of 3 g /L. This behaviour can be attributed to the increase of the surface covered θ (E_w %/100), and that due to the

adsorption of phytochemical components of the essential oil onto the mild steel surface resulting in the blocking of the reaction sites, and protection of this surface from the attack of the corrosion active ions in the acid medium. Consequently, we can conclude that the AG oil is a good corrosion inhibitor for mild steel in 0.5M H_2SO_4 solution.

Table 3. Gravimetric results of mild steel in acid without and with addition of the AG oil at various contents (*t*= 6h, *T*= 298 K).

Inhibitor	Concentration (g/L)	W (mg/h.cm2)	Ew (%)
H2SO4	0.5 M	1.79	--
	0.25	0.691	61.36
	0.5	0.606	66.13
AG oil	1	0.496	72.25
	1.5	0.408	77.18
	2	0.355	80.13
	3	0.306	82.89

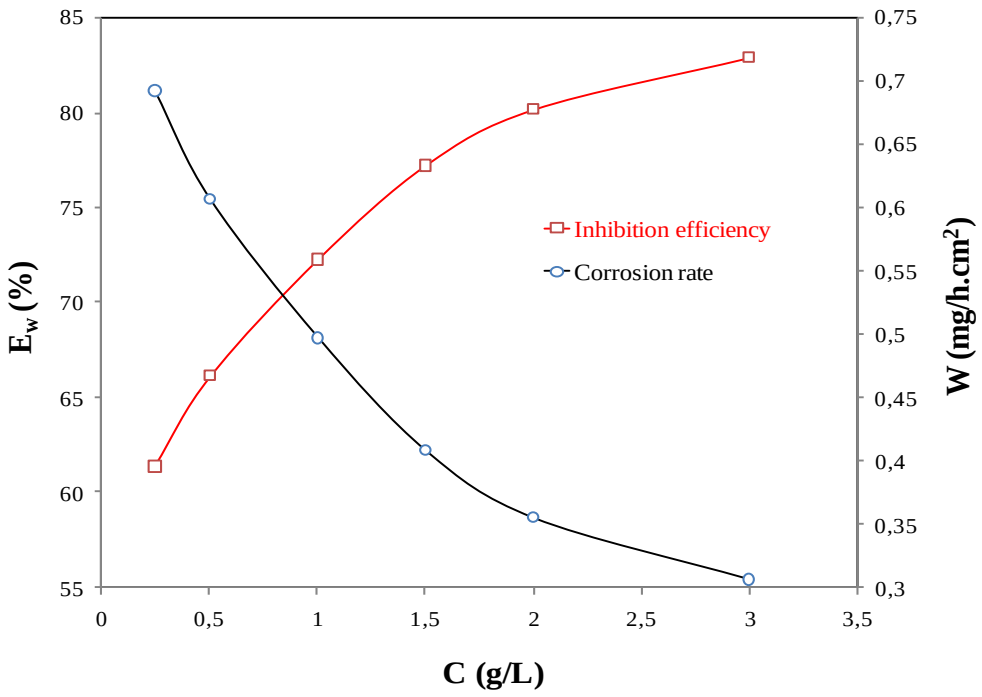

Figure 4. Variation of corrosion rate (W) and inhibition efficiency (Ew) of corrosion of mild steel in 0.5 M H_2SO_4 in the presence of AG oil.

In order to obtain a better understanding of the corrosion protection mechanism of AG oil against the corrosion of mild steel in normal sulphuric medium, a detailed study on this inhibitor was carried out using Tafel polarization and Electrochemical impedance spectroscopy (EIS) studies.

3.2.2. Polarization tests

Potentiodynamic anodic and cathodic polarization plots for mild steel specimens in 0.5M H_2SO_4 solution in the absence and presence of different concentrations of AG oil at 298 K are shown in Fig. 5. The respective kinetic parameters including corrosion current density (I_{corr}), corrosion potential (E_{corr}), cathodic and anodic Tafel slopes (βc, βa) and inhibition efficiency (IE%) are given in Table 4.

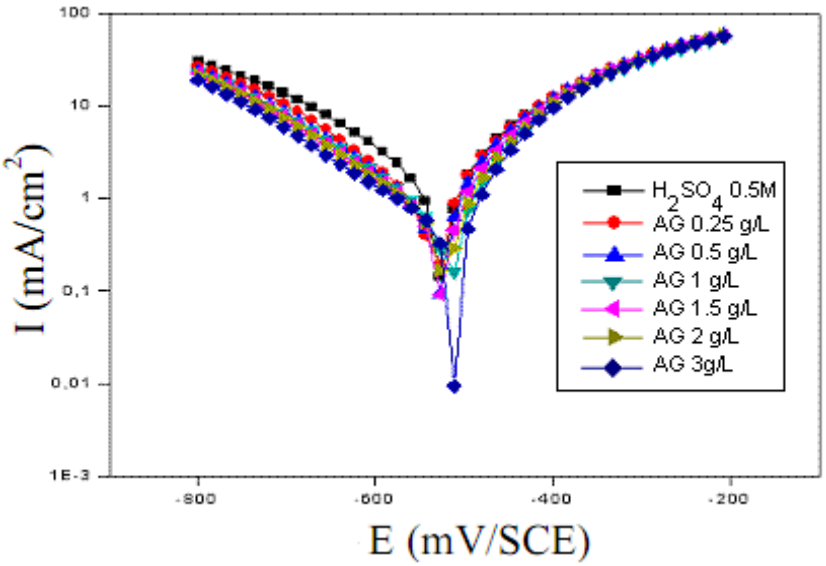

Figure 5. Polarization curves of mild steel in 0.5 M H_2SO_4 with and without AG oil at various concentrations at 298 K.

Table 4. Electrochemical parameters of mild steel at different concentrations of AG oil studied in 0.5 M H_2SO_4 at 298 K. Efficiencies corresponding corrosion inhibition.

Inhibitor	Concentration (g/L)	-Ecorr (mV)	Icorr (mA/cm²)	EI%	βa (mV)	-βc (mV)
	H2SO4 0.5M	576.7	2.6657	--	194.1	226.6
	0.25	576.2	1.6130	39.49	146.4	182.7
	0.5	576	1.3103	50.84	146.1	178.3
	1	574.2	1.1512	56.81	146	175.7
AG oil	1.5	576.2	1.1055	58.52	146	174
	2	574.9	1.0162	61.87	145.1	168.1
	3	574	0.8246	69.06	144.8	166.1

Inspection of Fig. 5 shows that the addition of AG oil has an inhibitive effect in the both anodic and cathodic parts of the polarization curves. Thus, addition of this inhibitor reduces the mild steel dissolution as well as retards the hydrogen evolution reaction. In addition, the parallel cathodic Tafel curves in Fig. 5 show that the hydrogen evolution is activation-controlled and the reduction mechanism is not affected by the presence of the inhibitor [29]. In the domain anodic (Fig. 5), the polarization curves of mild steel have shown that the addition of the essential oil decreases the current density. However, at potentials higher than -240 mV/sce, the presence of AG oil shows no effect on the anodic curves. This results suggest that the inhibitory action depends on the potential of inhibitor and a desorption process appears at high potential [30]. In this case, the desorption rate of the inhibitor is higher than its adsorption rate [31]. So, it could be concluded that this essential oil act as mixed type inhibitor for mild steel in 0.5 M H_2SO_4 solution.

The analyse of the data in Table 4 revealed that the corrosion current density (i_{corr}) decreases considerably with increasing AG oil concentration and moves the corrosion potential to positive values and βa changes in the presence of AG oil, which indicates that inhibitor molecule are pore adsorbed on the anodic sites resulting in an inhibition of the anodic reactions for mild steel in 0.5 M H_2SO_4 solution. The cathodic Tafel slope (βc) does not change upon addition of AG oil, which suggests that the inhibiting action occurred by simple blocking of the available cathodic sites on the metal surface, which lead to a decrease in the exposed area necessary for hydrogen evolution and lowered the dissolution rate with increasing natural oil concentration. The dependence of IE (%) versus the inhibitor concentration of AG oil is also presented in Table 4. The obtained efficiencies indicate that AG oil acts as a good corrosion inhibitor.

3.2.3. Electrochemical impedance spectroscopy (EIS)

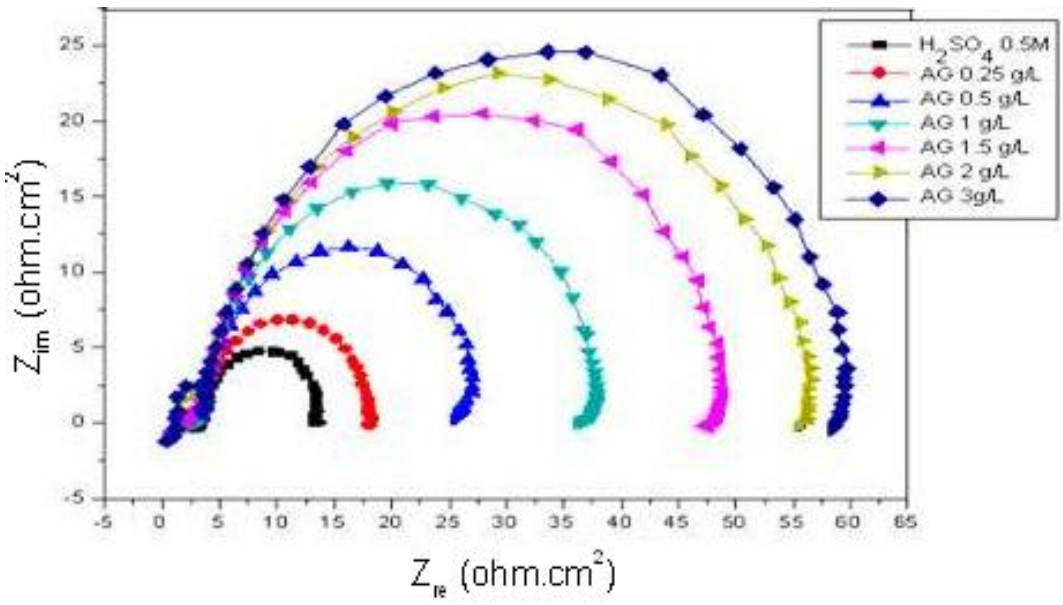

Figure 6. Nyquist plots of mild steel in 0.5 M H_2SO_4 containing various concentrations of AG oil

The corrosion behaviour of mild steel in 0.5 M H_2SO_4 solution, in the absence and presence of AG oil, is also investigated by the electrochemical impedance spectroscopy (EIS) at 298K after 30 min of immersion.

Impedance diagrams are obtained for frequency range 100 KHz –10 mHz at the open circuit potential for mild steel in 0.5 M H_2SO_4 in the presence and absence of AG oil. Nyquist plots for steel in 0.5 M H_2SO_4 at various concentrations of this oil are presented in Fig 6.

The EIS results are simulated by the equivalent circuit shown in Fig. 7 to pure electric models that could verify or rule out mechanistic models and enable the calculation of numerical values corresponding to the physical and/or chemical properties of the electrochemical system under investigation [32]. In the electrical equivalent circuit, R_s is the solution resistance, R_t the charge transfer resistance and C_{dl} is the double layer capacitance.

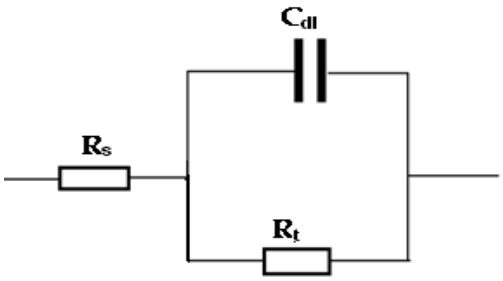

Figure 7. Equivalent circuit used to fit the EIS data of mild steel in 0.5 M H_2SO_4 without and with different concentrations of AG oil.

Table 5 gives values of charge transfer resistance, R_t double-layer capacitance, C_{dl}, and f_{max} derived from Nyquist plots and inhibition efficiency E_{Rt} (%°).

Table 5. Characteristic parameters evaluated from the impedance diagram for mild steel in 0.5 M H_2SO_4 at various concentrations of AG oil.

Inhibitor	Concentration (g/L)	-Ecorr (mV/SCE)	Rt (Ω.cm2)	F max (HZ)	Cdl (µF.cm2)	ERt%
	H2SO4 0.5M	572	10.53	316.46	3096	--
	0.25	574	15.04	200	1554	30
	0.5	576	25.07	158.23	523.8	58.36
AG oil	1	576	36.65	125	273.78	71.26
	1.5	567	46.35	100	171.58	77.19
	2	574	54.82	79.365	125.4	80.79
	3	576	57.45	63.291	112.64	81.67

The recorded EIS spectrum for mild steel in 0.5 M H_2SO_4 at 298 (Fig. 6) showed one single depressed capacitive loop. The same trend (one capacitive loop) was also noticed for mild steel immersed in 0.5 M H_2SO_4 containing AG oil (0.25–3g/L). The diameter of Nyquist plots increased on increasing the concentration of AG oil indicating strengthening of inhibitive film. Moreover, the single capacitive loop can be attributed to the charge transfer that takes place at electrode/solution interface, and the charge transfer process controls the corrosion reaction of mild steel and the presence of inhibitor does not change the mechanism of dissolution of mild steel [33]. It is also clear that these impedance diagrams are not perfect semicircles and this difference has been attributed to frequency dispersion [34] and has been attributed to roughness and other inhomogeneities of solid surface [35].

From the impedance data (Table 5), we conclude that the R_t values increase with inhibitor concentration and consequently the inhibition efficiency increases to 81.67% at 3g /L. In fact, the presence of AG oil is accompanied by the increase of the value of R_t in acidic solution confirming a charge transfer process mainly controlling the corrosion of mild steel. Values of double layer capacitance are also brought down to the maximum extent in the presence of inhibitor and the decrease in the values of C_{dl} follows the order similar to that obtained for I_{corr} in this study. The decrease in C_{dl} is due to the adsorption of the inhibitor on the metal surface leading to the formation of film or complex from acidic solution [36]. We also note the increase of the value of R_t with the inhibitor concentration leading to an increase in the corrosion inhibition efficiency.

The variation of inhibition efficiency (E %), determined by the three methods (weight loss, polarization curves and EIS methods), as a function of concentration of AG oil in 0.5 M H_2SO_4 was presented in Fig. 8. The results thus obtained show a good agreement with the three methods used in this investigation, significantly in high concentrations.

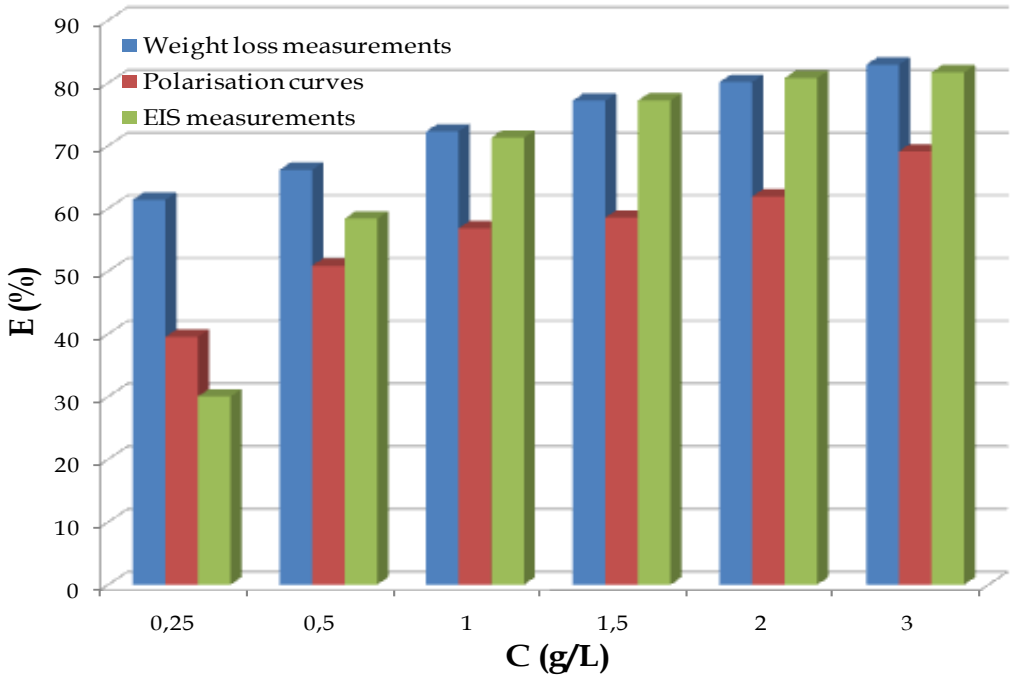

Figure 8. Comparison of inhibition efficiency (E%) values obtained by weight loss, polarization and EIS methods of mild steel in 0.5 M H_2SO_4 without and with different concentrations of AG oil.

3.3. Effect of temperature

The data of corrosion rates and corresponding efficiency (Ew) collected were presented in Table 6.

Table 6. Corrosion parameters obtained from weight loss for mild steel in 0.5 M H_2SO_4 containing 3 g/L of AG oil at different temperatures.

T (K)	Winh mg/cm2.h	W0 mg/cm2.h	Ew %
303	0.392	1.764	77.76
313	1.039	4.211	75.32
323	1.858	7.125	73.92
333	4.039	14.00	71.15
343	6.462	21.78	70.33

Examination of this Table reveals corrosion rate increases both in the uninhibited and inhibited acid solution with the rise of temperature. The presence of inhibitor leads to decrease of the corrosion rate. Also, we note that the efficiency (Ew %) depends on the temperature and decreases with the rise of temperature from 303 to 343 K. The decrease in inhibition efficiency with increase in temperature may be attributed to can be attributed to the increased desorption of inhibitor molecules from metal surface and the increase in the solubility of the protective film or the reaction products precipitated on the surface of the metal that might otherwise inhibit the reaction [37]. This is in accordance with the results reported by Ergun et al [38].

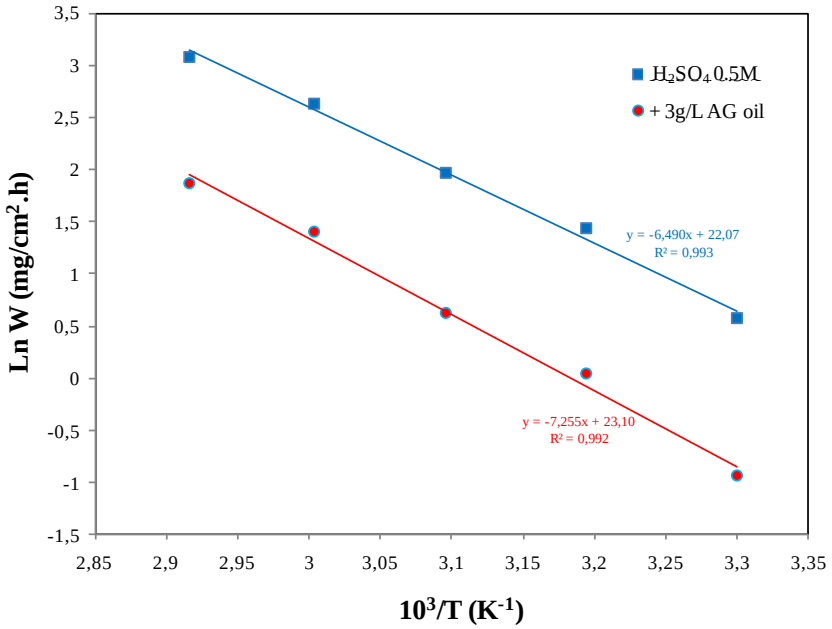

Figure 9. Arrhenius plots for mild steel corrosion rates (W) in 0.5 M H_2SO_4 in absence and in presence of 3 g/L of AG oil.

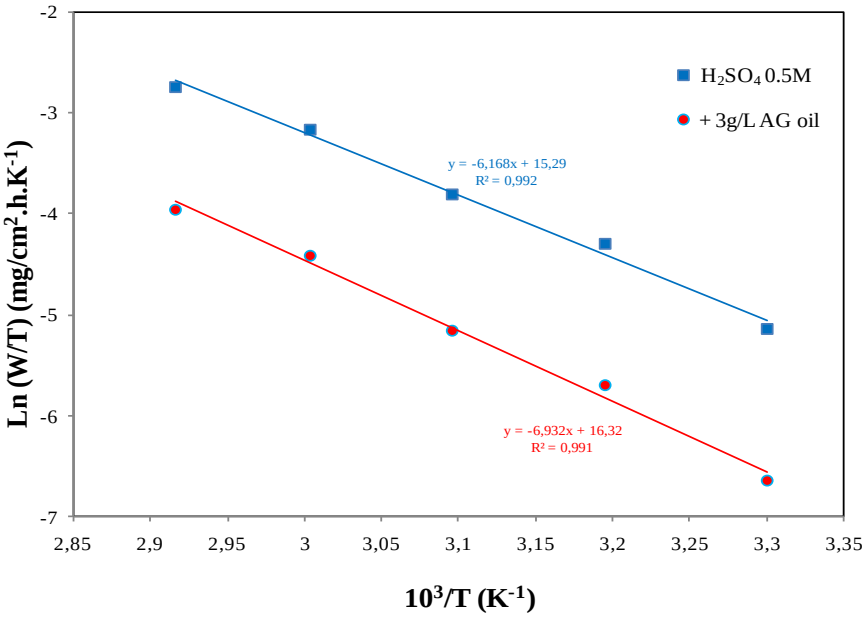

Figure 10. Transition-state plots for mild steel corrosion rates (W) in 0.5 M H_2SO_4 in absence and in presence of 3 g/L of AG oil.

The apparent activation energy (Ea) for mild steel in 0.5 M H_2SO_4 with the absence and presence of 3 g/L of AG oil were determined from the slopes of Ln (W) vs 1/T graph depicted in Fig. 9 and values are reported in Table 7.

Fig. 10 shows a plot of Ln (W/T) against 1/T. A straight lines are obtained with a slope of (-ΔH°a/R) and an intercept of (Ln R/Nh + ΔS°a/R) from which the values of ΔH°a and ΔS°a are calculated, are listed in Table 7.

Table 7. Corrosion kinetic parameters for mild steel in 0.5 M H_2SO_4 in the absence and presence of 3 g/L of AG oil.

Inhibitor	Ea (KJ. mol-1)	ΔH°a (KJ. mol-1)	Ea – ΔH°a (KJ. mol-1)	ΔS°a (J. mol-1.K-1)
H2SO4 0.5M	54	51.31	2.69	-70.39
+3 g/L AG oil	60.36	57.67	2.69	-61.81

The calculated values of activation energies from the slopes are 54 and 60.36kJ/mol for free acid and with the addition of 3 g/L of AG oil, respectively. We remark that the activation energy increases in the presence of inhibitor.

The higher Ea values, for inhibited solution than the uninhibited one, indicate that a strong inhibitive action of the additives by increasing energy barrier for the corrosion process, emphasizing the electrostatic character of the inhibitor's adsorption on the mild steel surface [39].

Moreover, inspection of the data of Table 7 reveals that the positive signs of $\Delta H°_a$ both in the absence and presence of 3 g/L of AG oil reflect the endothermic nature of the mild steel dissolution process suggesting that the dissolution of mild steel is slow [40].

The average difference value of the Ea – $\Delta H°_a$ is 2.69 kJ mol^{-1}, which is approximately equal to the average value of RT (2.69 kJ mol^{-1}) at the average temperature (323 K) of the domain studied. This result agrees that the corrosion process is a unimolecular reaction as described by the known Eq. (8) of perfect gas [41]:

$$E_a - \Delta H_a^{\circ} = RT \qquad (8)$$

On the other hand, the entropy of activation ($\Delta S°_a$) in the absence and presence of essential oil has large and negative values.

This indicates that the activated complex in the rate determining step represents an association rather than dissociation, meaning that a decrease in disordering takes place on going from reactants to the activated complex [42].

3.4. Adsorption isotherm

In order to acquire a better understanding of the adsorption mode of the inhibitor on the surface of the mild steel, the data obtained from the three different techniques were tested with several adsorption isotherms, including Langmuir, Frumkin, and Temkin.

The Langmuir isotherm(C/θ *vs* C) assumes that there is no interaction between adsorbed molecules on the surface. The Frumkin adsorption isotherm (θ *vs* C) assumes that there is some interaction between the adsorbates, and the Temkin adsorption isotherm (θ *vs* lgC) represents the effect of multiple layer coverage [43].

The dependence of the fraction of the surface covered θ obtained by the ratio E%/100 as function of the oil concentration (C_{inh}) was graphically fitted for various adsorption isotherms.

Fig. 11 shows the dependence of θ as function of the logarithm of oil concentration. The relationship between C/θ and C presents linear behaviour at 298 K with correlation factor equal to unity (0.998). This suggests that the adsorption of AG oil on mild metal surface followed the Langmuir adsorption isotherm. The Langmuir adsorption isotherm may be written in the following form:

$$\frac{C_{inh}}{\theta} = \frac{1}{b} + C_{inh} \qquad (9)$$

C_{inh} is the inhibitor concentration; θ is the fraction of the surface covered, b is the adsorption coefficient.

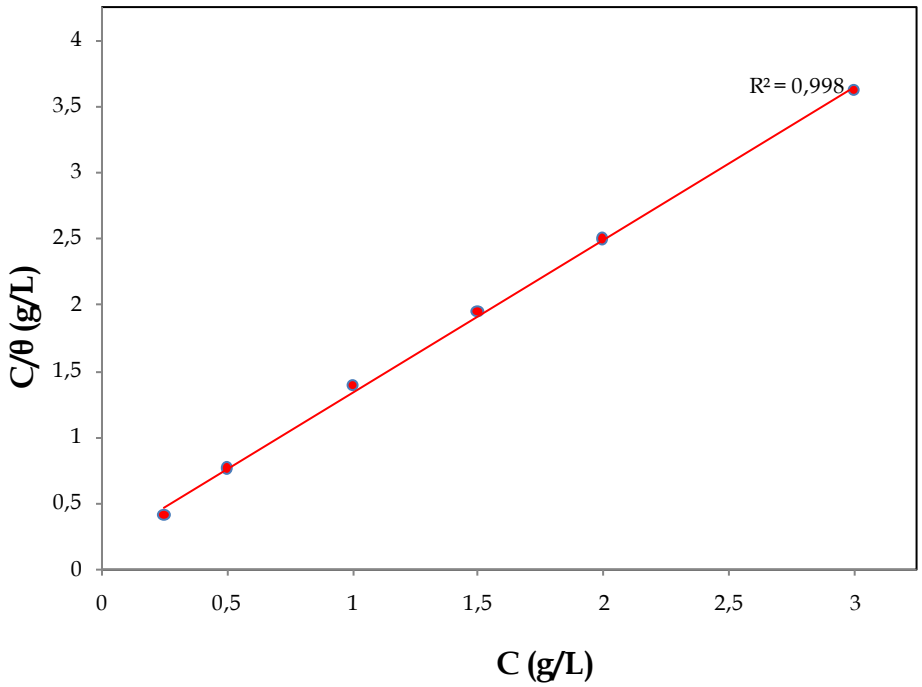

Figure 11. Langmuir adsorption isotherm of AG oil on the mild steel surface

3.5. Mechanism of inhibition

The gravimetric method, polarisation curves and electrochemical impedance spectroscopy confirms the inhibiting character of AG oil in acid solution. However, the inhibition efficiency increases with essential oil concentrations. This result suggests that the probable mechanism can be explained on the basis of adsorption process and the structure of the constituents present in the essential oil. The inhibition may be due to the adsorption of phytochemical constituents present in the oil by one and/or more of the following ways:

(1) electrostatic interaction of protonated molecules with already adsorbed sulphur ions;

(2) donor-acceptor interactions between the π-electrons of aromatic ring and vacant d orbital of surface iron atoms;

(3) interaction between unshared electron pairs of oxygen atoms and vacant d-orbital of iron surface atoms.

Generally, two modes of adsorption are considered on the metal surface in acid media. In one mode, the neutral molecules may be adsorbed on the surface of mild steel through the chemisorption mechanism, involving the displacement of water molecules from the mild steel surface and the sharing electrons between the oxygen atoms and iron. The inhibitor molecules can also adsorb on the mild steel surface on the basis of donor–acceptor interactions between π-electrons of the aromatic ring and vacant d-orbitals of surface iron atoms. In second mode, since it is well known that the mild steel surface bears positive charge in acid solution [44], it is difficult for the protonated molecules to approach the positively charged mild steel surface (H_3O^+/metal interface) due to the electrostatic repulsion. Since SO_4^{2-} have a smaller degree of hydration, they could bring excess negative charges in the vicinity of the interface and favour more adsorption of the positively charged inhibitor molecules,

the protonated inhibitors adsorb through electrostatic interactions between the positively charged molecules and the negatively charged metal surface. Thus, there is a synergism between adsorbed SO_4^{2-} ions and protonated inhibitors. Thus, inhibition of mild steel corrosion in 0.5 M H_2SO_4 is due to the adsorption of phytochemical constituents on the mild steel surface [45,46].

Presumably, the adsorption of *A. graveolens* essential oil is probably made by 6-oxocyclonerolidol and 6-hydroxycyclonerolidol which were the main components. However, a synergistic or antagonistic effect of other molecules may play an important role on the inhibition efficiency of this oil.

4. CONCLUSIONS

The study of chemical composition and effect of *Asteriscus graveolens* essential oil on the corrosion of mild steel in 0.5 M H_2SO_4 conducted by weight loss measurements and electrochemical method may draw the following conclusions:

(1) Chemical analysis shows 6-oxocyclonerolidol and 6-hydroxycyclonerolidol are the major components of *Asteriscus graveolens* essential oil with (74.9%) and (11.8%) respectively;

(2) Inhibition efficiency increases with the concentration of inhibitor and decreases with temperature;

(3) *Asteriscus graveolens* essential oil acts as good inhibitor for the corrosion of mild steel in 0.5 M H_2SO_4 with an inhibition efficiency 82.89% at 3g/L;

(4) The natural oil acts on mild steel surface in 0.5 M H_2SO_4 solution as mixed type inhibitor with a strong predominance of anodic character;

(5) Inhibition efficiency on mild steel may occur by action of 6-oxocyclonerolidol and 6-hydroxycyclonerolidol probably.

References

1. G. Blustein, J. Rodriguez, R. Romanogli, C.F. Zinola, *Corros. Sci*. 47 (2005) 369
2. M.A. Amin, K.F. Khaled, Q. Mohsen, H.A. Arida, *Corros. Sci*. 52 (2010) 1684.
3. N.O. Eddy, EE. Ebenso, *Afr. J. Pure Appl. Chem*. 2 (2008) 46.
4. S. Bilgic, *Korozyon* 13 (2005) 3.
5. M. Znini, L. Majidi, A. Bouyanzer, J. Paolini, J.M. Desjobert, J. Costa, B. Hammouti, *Arab. J. Chem*. (2010), doi: 10.1016/j.arabjc.2010.09.017
6. M. Znini, M. Bouklah, L. Majidi, S. Kharchouf, A. Aouniti, A. Bouyanzer, B. Hammouti, J. Costa, S.S. Al-Deyab, *Int. J. Electrochem. Sci*. 6 (2011) 691.
7. M. Znini, L. Majidi, A. Laghchimi, J. Paolini, B. Hammouti, J. Costa, A. Bouyanzer, S. S. Al-Deyab, *Int. J. Electrochem. Sci*. 6 (2011) 5940.
8. M. Znini, J. Paolini, L. Majidi, J.-M. Desjobert, J. Costa, N. Lahhit, A. Bouyanzer, *Res. Chem. Intermed*. 38 (2012) 669.

9. G. Cristofari, M. Znini, L. Majidi, A. Bouyanzer, S.S. Al-Deyab, J. Paolini, B. Hammouti, J. Costa, *Int. J. Electrochem. Sci*. 6 (2011) 6699.
10. A. Bouyanzer, B. Hammouti, L. Majidi, *Mat. Lett*. 60 (2006) 2840.
11. A. Bouyanzer, L. Majidi, B. Hammouti, *Bull. Electrochem*. 22 (2006) 321.
12. O. Ouachikh, A. Bouyanzer, M. Bouklah, J-M. Desjobert, J. Costa. B. Hammouti, L. Majidi, *Surf. Rev. Lett*. 16 (2009) 49.
13. A. Bouyanzer, L. Majidi, B. Hammouti, *Phys. Chem. News*. 37 (2007) 70.
14. N. Lahhit, A. Bouyanzer, J.M. Desjobert, B. Hammouti, R. Salghi, J. Costa, C. Jama, F. Bentiss, F, L. Majidi, *Portug. Electrochim. Acta* 29 (2011) 127.
15. A. Cheriti, A. Saad , N. Belboukhari, S. Ghezali, *Flav. Frag. J*. 22 (2007) 286.
16. H. Fahmy, *J. Eviron. Sci*. 26 (2003) 307.
17. A. Benchelah, H. Bouziane, M. Maka, *Phytothrapie*, 6 (2004) 191.
18. M. Znini, G. Cristofari, L. Majidi, H. Mazouz, P. Tomi, J. Paolini, J. Costa, *Nat. Prod. Comm*. 6 (2011) 1763.
19. S. Youssef, Z. Ibraheim, A. Attia, *Pharm. Sci. Assiut. Univ*. 18 (1995) 33.
20. T. Sarg, S. El-Dahmy, A. Ateya, H. Abdel-Fattah, *Fitoterapia*, 5 (1994) 179.
21. European Pharmacopoeia, "Council of Europe". Strasbourg, 3rd ed, (1997) 121.
22. H. Dool, P. Kratz, *J. Chromatogr*. 11 (1963) 463.
23. D. Joulain, König, W.A., The atlas of spectral data of sesquiterpene hydrocarbons. EbVerlag Hamburg. (1998).
24. D. Hochmuth, D. Joulain, König, W.A., Terpenoids and related constituents of essential oils, Library of Massfinder 2. 1 University of Hamburg Institute of organic chemistry Hamburg Germany. (2001).
25. R.P. Adams, Identification of Essential Oil Components by Gaz Chromatography/Quadrupole Mass Spectroscopy. Allured Publishing: Carol Stream. (2004).
26. C. Bicchi, E. Liberto, M. Matteodo, B. Sgorbini, L. Mondello, B.A. Zellner, R. Costa et al,. *Flav. Frag. J*. 23 (2008) 382.
27. S.H. Tsuru, B. Gijutsu, *J. Jpn. Soc. Corros. Eng*. 27 (1978) 573.
28. F. Bentiss, M. Lebrini, M. Lagrenée, *Corros. Sci*. 47 (2005) 2915.
29. J.O.M. Bockris, B. Young, *J. Electrochem. Soc*. 138 (1999) 2237.
30. M. Bouklah, N. Benchat, A. Aouniti, B. Hammouti, M. Benkaddour, M. Lagrenée, H. Vezine, F. Bentiss, *Prog. Org. Coat*. 51 (2004) 118.
31. F. Bentiss, M. Traisnel, N. Chaibi, B. Mernari, H. Vezin, M. Lagrenée, *Corros. Sci*. 44 (2002) 2271.
32. M. Benabdellah, A. Aouniti, A. Dafali, B. Hammouti, M. Benkaddour, A. Yahyi, A. Ettouhami, *Appl. Surf. Sci*. 252 (2006) 8341.
33. A.R.S. Priya, V.S. Muralidharam, A. Subramanian, *Corrosion*, 64 (2008) 541.
34. Y. Larabi, M. Harek, M. Traisnel, A. Mansri, *J. Appl. Electrochem*. 34 (2004) 833.
35. F. Mansfeld, M.W. Kending, S. Tsai, *Corrosion*. 38 (1982) 570.
36. K. Juttner, *Electrochim. Acta*. 35 (1990) 1501.
37. M. Lagrenée, B. Mernari, M. Bouanis, M. Traisnel, F. Bentiss, *Corros. Sci*. 44 (2002) 573.
38. E.E. Ebenso, Hailemichael Alemu, S.A. Umoren, I.B. Obot, *Int. J. Electrochem*. Sci. 3 (2008) 1325.
39. U. Ergun, D. Yuzer, K.C. Emergul, *Mater. Chem. Phy*.109 (2008) 492.
40. M.I. Awad, *J. Appl. Electrochem*. 36 (2006) 1163
41. N.M. Guan, L. Xueming, L. Fei, *Mater. Chem. Phys*. 86 (2004) 59.
42. M.K. Gomma, M.H. Wahdan, *Mater. Chem. Phys*. 39 (1995) 209.
43. S. Samkarapapaavinasam, M.F. Ahmed, *J. Appl. Electrochem*. 22 (1992) 390.
44. N. Labjar, M. Lebrini, F. Bentiss, N. Chihib, S. El Hajjaji, C. Jama, *Mater. Chem. Phys*. 119 (2010) 330.

45. G.N. Mu, T.P. Zhao, M. Liu, T. Gu, *Corrosion*. 52 (1996) 853.
46. I. Ahamad, S. Khan, K.R. Ansari, M.A. Quraishi, *J. Chem. Pharm. Res*. 3 (2011) 703.
47. A. Singh, V.K. Singh, M.A. Quraish, *J. Mater. Environ. Sci*. 1 (2010) 162.